Research on Orbital Angular Momentum Different Modes Networking Method in Wireless Communication

Zishen Zhu, Chengyu Zhang, Luhan Wang, Wei Zheng, *Member, IEEE*, and Xiangming Wen, *Senior Member, IEEE*

***Abstract*—Orbital angular momentum (OAM) has been a popular topic due to the natural orthogonality of OAM waves with different modes. It is expected to greatly improve the channel capacity of wireless communication systems. From the perspective of networking, this letter proposes an OAM-based different modes networking method (OAM DMN) that sets adjacent cells with OAM carriers of different modes, so as to improve the signal quality and spectrum efficiency of wireless network and better adapt to the high-density base station distribution scenario. This letter firstly analyzes the characteristics of atmospheric channel on OAM waves by regarding turbulent as random phase screen based on Kolmogorov turbulence theory. Combining with stochastic geometry, we get the outage probability function of wireless cells. Then two types of OAM DMN schemes are proposed to test the performance of the network under different channel conditions. Simulation shows that OAM DMN wireless network has lower outage probability compared with other OAM-based and conventional networks and better performance on high-density base station distribution.**

***Index Terms*—Orbital angular momentum, mobile communication, different modes networking, atmospheric turbulence.**

I. Introduction

THE ORBITAL angular momentum wave has a spiral wavefront $\exp(-il\phi)$ whose shape is determined by mode l, where l can take any integer [1]. OAM waves with different modes are naturally orthogonal, which leads to a new dimension for the multiplexing of wireless communication [2]. The OAM-based mode division multiplexing method (OAM MDM) has been widely studied in the field of wireless communication which is a controversial topic. Zhao *et al.* [3], showed that OAM MDM is not an optimal technique for realizing the capacity limits of a free-space communication channel, and is outperformed by both conventional multiple-input-multiple-output (MIMO) transmission and spatial mode multiplexing (SMM). But with experiment, Ren *et al.* [4], demonstrated a 16 Gbps millimeter-wave link by combining OAM multiplexing with conventional spatial multiplexing. The scheme of OAM with index modulation was proposed in [5] to improve error performance and achieve high energy efficiency. The joint multiplexing between OAM MDM and orthogonal frequency division multiplexing applied in MIMO system achieved a very high sum-rate and spectrum efficiency [6].

However, in atmospheric channel, turbulence makes the refractive index of atmosphere non-uniform that distorts the propagating radio wave [7]. Therefore, when OAM waves propagate in atmospheric turbulence, helical phase distortion will occur, resulting in the loss of orthogonality. Thus, OAM wave of mode l can be expanded to $\{-\infty, \ldots, l-2, l-1, l, l+1, l+2, \ldots, +\infty\}$ for mixed mode waves. Based on Kolmogorov turbulence theory, in [8], Lou *et al.* used Rytov approximation and quadratic approximation of spherical waves [9] for OAM waves to simplify atmospheric turbulence into multiplicative phase noise. A unified statistical model for atmospheric turbulence-Induced fading in OAM-based free space optical (FSO) systems was proposed in [10], where the authors used Generalized Gamma distribution to model the crosstalk between OAM modes. Bedir *et al.* [11] and Yousif and Elsayed [12] proposed an adaptive MIMO-FSO links using an OAM-multiplexed based on the SMM combined with an adaptive MIMO technique, and used SMM and modified pulse position modulation in hybrid RF/FSO OAM-MIMO multiplexed to mitigate the atmospheric turbulence effects.

Most research have ignored the application of OAM in networking. As the scale of wireless networks gradually increases, co-frequency networking [13] and inter-frequency networking [14] methods face the challenges of meeting the wireless network's demand for high-density base station distribution scenario. Co-frequency networking introduces co-frequency interference between cells thus reduces signal quality, while inter-frequency networking gets low frequency band efficiency. The orthogonality of OAM waves is independent of frequency band, which provides a new method about networking.

In this letter, the application of OAM technique in networking of wireless network has been investigated. The contributions of this letter are summarized as follows.

(1) An OAM-based different modes networking method (OAM DMN) for wireless network is proposed, which sets adjacent cells with OAM carriers of different modes to send cell signal.

(2) A new random atmospheric channel model is proposed by combining amplitude fading and spiral phase distortion, where we directly change the influence of atmospheric

Manuscript received January 2, 2022; revised February 14, 2022; accepted February 14, 2022. Date of publication February 18, 2022; date of current version May 10, 2022. This work was supported in part by the National Key Research and Development Program of China under Project 2019YFB1803303, and in part by Beijing Natural Science Foundation under Grant L202002. The associate editor coordinating the review of this article and approving it for publication was D. B. da Costa. *(Corresponding author: Wei Zheng.)*

The authors are with the Beijing Key Laboratory for Network System Architecture and Convergence, Beijing Laboratory of Advanced Information Networks, Beijing University of Posts and Telecommunications, Beijing 100876, China (e-mail: zhengweius@bupt.edu.cn).

Digital Object Identifier 10.1109/LWC.2022.3152735

turbulence on OAM spiral phase fluctuations into a random phase screen by using inversion method [15], based on Kolmogorov's atmospheric turbulence theory. Furthermore, we get the outage probability function of wireless cells by combining stochastic base station distribution and random atmospheric channel model.

(3) Two types of OAM DMN schemes are proposed to compare with relate work in OAM and networking. By contrast, simulation results show that OAM DMN gets better performance on signal quality and adapting to high-density base station scenarios.

II. System Model

In this letter, we research on downlink communication where the base station sends OAM waves in all directions to cover the entire cell. Under cylindrical coordinate system, with the signal propagation direction as the z-axis, the signal transmitted in cell *n* can be expressed as

$$U_n(r,\phi,t) = s_n(t) f_n(r)\exp(-il_n\phi) \tag{1}$$

where ϕ and r represents the azimuth angle and radius, respectively. $s_n(t)$ is the information sent by cell n and $f_n(r)\exp(-il_n\phi)$ is a normalized OAM carrier of mode l_n with the following properties:

$$\iint f_n(r)\exp(-il_n\phi) f_m(r)\exp(il_m\phi) r dr d\phi = \begin{cases} 0 & l_m = l_n \\ 1 & l_m \neq l_n \end{cases} \tag{2}$$

Considering the divergence of OAM waves [16] and the limits on the number of neighbor cells, we choose to send normalized OAM carriers in low modes to ensure similar characteristics among carriers of different modes.

OAM waves of neighboring cells of cell *n* will undergo mode expansion to contain the harmonics of the l_n mode OAM wave, due to helical phase distortion caused by turbulence, which introduce inter-mode interference to cell *n*. Thus, users choose to connect to the nearest base station while still receive interference signals from adjacent cells. Meanwhile, carriers will be affected by amplitude fading resulting from propagation effects.

Next, we will establish models of base station distribution and atmospheric channel for specific analysis.

A. Base Station Distribution

Taking the randomness of base station location into account, we model the distribution of base stations as a two-dimensional Poisson distribution, which can be expressed as follow

$$\Pr\left[N(M') = m\right] = \left[\lambda S(M')\right]^m \exp\left(\frac{-\lambda S(M')}{m!}\right) \tag{3}$$

where M' represents the plane of base stations, $N(M')$ denotes the number of base stations on M', $S(M')$ is the area of M' and λ is the density constant of Poisson points distribution. We use the Voronoi-Poisson model to divide the cells as shown in Fig. 1. Thereby, we can get the probability density function of the distance distribution between user and the nearest base station as [17]

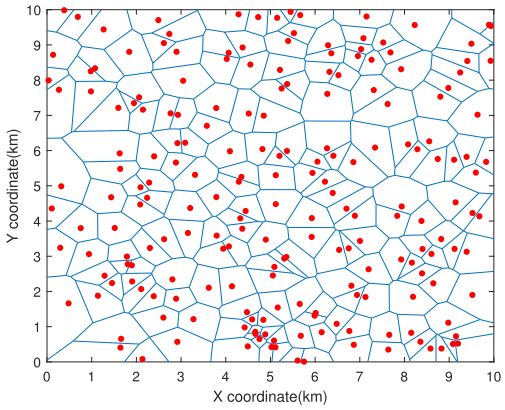

Fig. 1. Poisson distribution base station and cells divided according to the Voronoi-Poisson model.

$$f_z(z) = \exp(-\lambda\pi z^2)2\pi\lambda z. \tag{4}$$

B. Channel Model

In this section, we will model the atmospheric channel and discuss the magnitude of amplitude fading and inter-mode interference.

Usually, we use UCA [18] to generate radio OAM waves by combining multiple spheric waves. So, amplitude fading followed by spherical waves in free space is also applicable to OAM waves [8].

As far as random channel effects such as fading and shadowing, the standard power loss propagation model can be divided into large-scale fading and small-scale fading. We use $z^{-\alpha}$ to represent the large-scale fading, where z is the propagation distance and α represents the fading factor. According to [15], we assume that Rayleigh fading with mean 1 and constant transmit power of $1/\mu$ are experienced between base station and user. In summary, the amplitude fading of OAM waves propagated in free space is $hz^{-\alpha}$. The random variable h follows an exponential distribution with mean $1/\mu$, which can be denoted as $h \sim \exp(\mu)$.

Ignoring the impact of turbulence on amplitude, next, we will discuss the influence of turbulence on phase fluctuation of OAM wavefront.

In this letter, Kolmogorov turbulence theory is used to approximate the turbulence experienced by OAM wave transmission, which matches the near-surface environments [9]. The refraction power spectrum of the modified von Karman model is as follow:

$$\Phi_n(k) = 0.033 C_n^2 \frac{exp(k^2/k_l^2)}{(k^2+k_0^2)^{11/6}} \tag{5}$$

In (5), k represents the spatial wave number, and C_n^2 is the atmospheric structure constant. $k_l = 2\pi/L_0$ and $k_0 = 5.92/l_0$, where L_0 and l_0 denote the turbulence outer and inner scale, respectively. C_n^2 is affected by temperature and humidity in near-surface environments which is also related to frequency.

We use inversion method to convert the turbulence into a phase grating [15]. First, converting the refraction power spectrum to the phase power spectrum $\Phi_\phi(f)$:

$$\Phi_\phi(f) = 0.023 r_0^{-\frac{5}{3}} \frac{\exp(-f^2/f_l^2)}{(f^2+f_0^2)^{11/6}} \tag{6}$$

In (6), $f = k/2\pi$ is the spatial frequency, and $r_0 = [0.423k^2 z C_n^2]^{-\frac{3}{5}}$ is the atmospheric space radius. Then, we randomly generate a complex Gaussian matrix $h(k_x, k_y)$, with a mean of 0 and a variance of 1, to calculate the random phase screen as

$$\psi(r,\phi,\phi_{AT}) = Re\{\mathbb{F}^{-1}[h(k_x,k_y)\sqrt{\Phi_\phi(f)}]\} \tag{7}$$

where $\mathbb{F}^{-1}(\cdot)$ denotes the inverse fourier transform.

In summary, we take the turbulent phase interference as multiplicative phase noise of $\exp(-i\psi(r,\phi,\phi_{AT}))$, where $\psi(r,\phi,\phi_{AT})$ is a plane random process, and ϕ_{AT} is a phase random variable. While the plane coordinate (r,ϕ) is determined, ψ can be expressed as a random variable, and with certain value of ϕ_{AT}, ψ can be expressed as a certain phase screen on the plane. Therefore, after passing through turbulence, the transmitted wave can be written as

$$U_n^{TU}(r,\phi,t) = s_n(t) f_n(r) \exp(-il_n\phi) \exp(-i\psi(r,\phi,\phi_{AT})) \tag{8}$$

Performing harmonic expansion on $U_n^{TU}(r,\phi,t)$, we can give that:

$$U_n^{TU}(r,\phi,t) = \frac{1}{\sqrt{2\pi}} \sum_{-\infty}^{+\infty} s_n(t) a_{nk}(r) \exp(-il_k\phi) \tag{9}$$

$$a_{nk}(r) = \frac{1}{\sqrt{2\pi}} \int_0^{2\pi} U_n^{TU}(r,\phi,t) \exp(il_k\phi) d\phi \tag{10}$$

Suppose the energy of the harmonic with the mode *k* in the wave is C_{nk}.

$$\begin{aligned} C_{nk} &= \int_0^{+\infty} |a_{nk}(r)|^2 r dr \\ &= \int_0^{+\infty} \frac{|f_n(r)|^2}{2\pi} \iint exp(i(l_k - l_n)(\ phi i_1 - \phi_2)) \\ &\quad \times \exp(-i(\psi(r,\phi_1,\phi_{AT}) - \psi(r,\phi_2,\phi_{AT}))) d\phi_1 d\phi_2 r dr \end{aligned} \tag{11}$$

Let β_{nk} denotes the energy proportion of the harmonic, it can be expressed as

$$\beta_{nk} = \frac{C_{nk}}{\sum_{j=-\infty}^{+\infty} C_{nj}}. \tag{12}$$

Fig. 2 shows the mode expansion of OAM waves after propagating through turbulence. Through (a) and (b), it can be concluded that the larger the interval between harmonic mode and propagation mode, the smaller the magnitude of harmonic component. Comparing (b), (c) and (d), the magnitude of the harmonic component is positively correlated with propagation distance and intensity of turbulence. When $C_n^2 = 10^{-10} m^{-\frac{2}{3}}$, OAM waves occur serious mode expansion resulting that the energy of each harmonic will have a similar proportion.

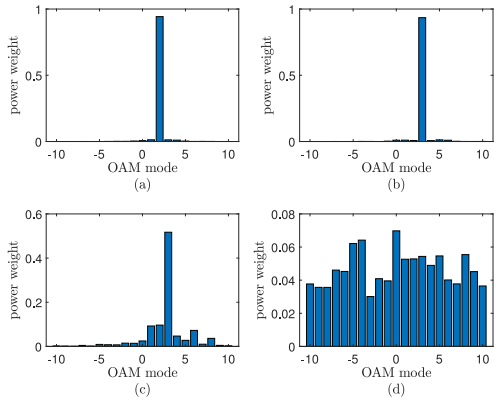

Fig. 2. Mode expansion of OAM waves of different modes through kinds of turbulence and propagation distance. (a) $l = 2$, $C_n^2 = 10^{-12} m^{-\frac{2}{3}}$, $z = 100m$. (b) $l = 3$, $C_n^2 = 10^{-12} m^{-\frac{2}{3}}$, $z = 100m$. (c) $l = 3$, $C_n^2 = 10^{-12} m^{-\frac{2}{3}}$, $z = 1000m$. (d) $l = 3$, $C_n^2 = 10^{-10} m^{-\frac{2}{3}}$, $z = 100m$.

III. Evaluation Model

In this section, we use outage probability as an indicator to evaluate the signal quality of OAM-DMN wireless network. When the SINR is less than a certain threshold, the connection will be interrupted. In downlink communication, users in cell *n* only demodulate OAM signals of mode l_n, which means that the users are only interfered by the harmonic component of mode l_n from neighboring cells. We suppose that additive white Gaussian noise, with a mean value of 0 and a variance of σ^2, will be superimposed in the atmospheric channel. The SINR of cell *n* can be obtained as

$$\gamma_n = \frac{h z_n^{-\alpha} \beta_{nn}}{\sigma^2 + I_n} \tag{13}$$

where $I_n = \sum_{m \in M \setminus n} h z_m^{-\alpha} \beta_{mn}$ represents the inter-mode interference and z_m denotes the distance between the user and the base station of cell *m*.

Assuming that the SINR threshold of cell *n* is *T*. According to the definition of outage probability:

$$\Pr_n^{out} = \Pr(\gamma_n < T) = 1 - \Pr(\gamma_n > T) \tag{14}$$

$$\begin{aligned} \Pr(\gamma_n > T) &= \mathbb{E}_{z_n}[\Pr(\gamma_n > T | z_n)] \\ &= \int_{z_n>0} \Pr(\gamma_n > T | z_n) \exp(-\pi\lambda z_n^2) 2\pi\lambda z_n dz_n \end{aligned} \tag{15}$$

$$\Pr(\gamma_n > T | z_n) = \Pr(h > (I_n + \sigma^2) z_n^\alpha \beta_{nn}^{-1} T | z_n) \tag{16}$$

Therefore, the expression of outage probability is

$$\begin{aligned} \Pr_n^{out} = 1 - \int_{z_n>0} &\Pr(h > (I_n + \sigma^2) z_n^\alpha \beta_{nn}^{-1} T | z_n) \\ &\times \exp(-\pi\lambda z_n^2) 2\pi\lambda z_n dz_n. \end{aligned} \tag{17}$$

IV. Simulation

First, we simplify the expression of β_{nk} as it is too complicated to perform numerical analysis. According to (6) and (7), the following conversion can be performed:

$$\psi(r,\phi,\phi_{AT}) = \sqrt{z} Re\mathbb{F}^{-1}[h(k_x,k_y)\sqrt{\frac{\Phi_\phi(f)}{z}}] \tag{18}$$

We set $\psi'(r,\phi,\phi_{AT}) = \psi(r,\phi,\phi_{AT})/\sqrt{z}$, where ψ' is independent of z. So, the superimposed phase noise in (8) can be rewritten as $\exp(-i\sqrt{z}\psi'(r,\phi,\phi_{AT}))$.

In (7), the $h(k_x,k_y)$ is random. With different $h(k_x,k_y)$, we calculate the outage probability for every matrix and take the average as the final result. Therefore, for each certain complex Gaussian matrix, there is:

$$\exp(-i\psi(r,\phi,\phi_{AT})) = \exp(-i\sqrt{z}\psi'(r,\phi)) \tag{19}$$

In (19), ψ' is a certain function. Bring ψ' in (11):

$$C_{nk} = \int_0^{+\infty} \frac{|f_n(r)|^2}{2\pi} \iint \exp(i(l_k - l_n)(\phi_1 - \phi_2)) \times \exp(-i\sqrt{z_n}(\psi'(r,\phi_1) - \psi'(r,\phi_2)))d\phi_1 d\phi_2 r dr \tag{20}$$

Therefore, C_{nk} is a random variable determined by z_n. According to (12), β_{nk} is determined by z_n, similarly. So, formula (16) can be solved as following:

$$\begin{aligned}\Pr(\gamma_n > T|z_n) &= \mathbb{E}_{I_n}[\Pr(h > (I_n+\sigma^2)z_n^{\alpha}\beta_{nn}^{-1}T|z_n,\beta_{nn}] \\ &= \mathbb{E}_{I_n}[\exp(-\mu(I_n+\sigma^2)z_n^{\alpha}\beta_{nn}^{-1}T|z_n)] \\ &= \exp(-\mu\sigma^2 z_n^{\alpha}\beta_{nn}^{-1}T)\mathbb{E}_{I_n}[\exp(-\mu I_n z_n^{\alpha}\beta_{nn}^{-1}T)]\end{aligned} \tag{21}$$

Combining [17] and the above derivation, we can get

$$\begin{aligned}&\mathbb{E}_{I_n}[\exp(-\mu I_n z_n^{\alpha}\beta_{nn}^{-1}T)] \\ &= \mathbb{E}_{\Phi}[\prod_{m\in M\setminus n}\mathbb{E}_h[\exp(-\mu z_n^{\alpha}\beta_{nn}^{-1}Th\beta_{mn}z_m^{-\alpha})]] \\ &= \exp(-2\pi\lambda\int_{z_n}^{+\infty}(1-\mathbb{E}_h[\exp(-\mu z_n^{\alpha}\beta_{nn}^{-1}Th\beta_{mn}(v)v^{-\alpha})])vdv) \\ &= \exp(-2\pi\lambda\int_0^{+\infty}(\int_r^{+\infty}(1-\exp(-\mu z_n^{\alpha}\beta_{nn}^{-1}Th\beta_{mn}(v)v^{-\alpha})) \\ &\quad \cdot vdv)f(h)dh)\end{aligned} \tag{22}$$

In summary, we can get the outage probability as

$$\begin{aligned}\Pr_{out} = 1 - \int_{r>0}&\exp(-\mu\sigma^2 z_n^{\alpha}\beta_{nn}^{-1}T)\exp(-2\pi\lambda\int_0^{+\infty} \\ &(\int_{z_n}^{+\infty}(1-\exp(-\mu z_n^{\alpha}\beta_{nn}^{-1}Th\beta_{mn}(v)v^{-\alpha}))vdv)f(h)dh) \\ &\cdot\exp(-\pi\lambda z_n^2)2\pi\lambda z_n dz_n\end{aligned} \tag{23}$$

Two OAM DMN schemes are proposed to compared with two baselines summarized as follows:

SCHEME 1: First, sorts the neighboring cells of cell n, according to the distance between user and the base stations from large to small, and then assigns a mode of $l_n + j, j \in (1, 2\cdots)$ to neighboring cells in turn, where j is the sorted serial number about cells. Scheme 1 can maximize the allocation of applicable modes to different cells. Furthermore, neighboring cell chooses smaller mode difference with cell n, with larger distance to user. The interference is greater with smaller mode interval and distance. Therefore, in this way, we can reduce the interference brought by cells with smaller mode interval.

SCHEME 2: Assigns a mode of $l_n + 2j, j \in (1, 2\cdots)$ to neighboring sorted cells, similar to scheme 1 in turn.

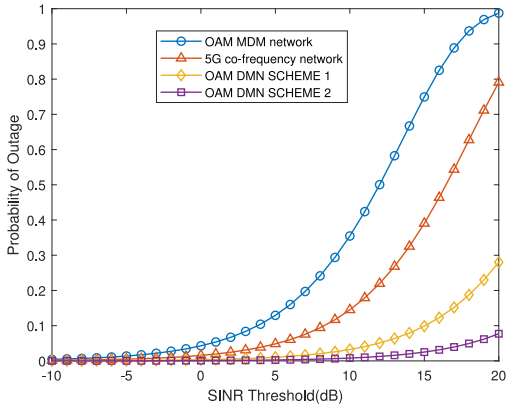

Fig. 3. Simulation results for outage probability of different schemes. $\lambda = 2/km^2$, $C_n^2 = 1\times10^{-12}m^{-\frac{2}{3}}$.

Larger mode interval can further reduce the interference received by cell n. Due to the limitation of numbers of adjacent cells, we could still allocate modes within the scope of available modes.

BASELINE 1: In 5G wireless downlink network, co-frequency networking method is used to achieve higher band utilization with beamforming to improve the quality of received signals of user [19]. We abstract the effect of beamforming of cell n as a power factor B_n. The SINR of cell n can be expressed as $\gamma_n = B_n h z_n^{-\alpha}/(\sigma^2 + I_n)$. Therefore, the outage probability of baseline 1 can be written as

$$\begin{aligned}\Pr_{out} = 1 - \int_{r>0}&\exp(-\mu\sigma^2 z_n^{\alpha}B_n^{-1}T)\exp(-2\pi\lambda\int_0^{+\infty} \\ &(\int_{z_n}^{+\infty}(1-\exp(-\mu z_n^{\alpha}B_n^{-1}Thv^{-\alpha}))vdv)f(h)dh) \\ &\cdot\exp(-\pi\lambda z_n^2)2\pi\lambda z_n dz_n\end{aligned} \tag{24}$$

BASELINE 2: In OAM MDM network, kinds of modes are used in one cell. Taking the limitation of available low modes into account, different cells will share the same mode. So, the SINR can be modified into $\gamma_n = hz_n^{-\alpha}\beta_{nn}/(\sigma^2 + I_n^1 + I_n^2)$ where I_n^1 and I_n^2 denotes interference from cell n and neighboring cell. Therefore, it is easy to get:

$$\begin{aligned}\Pr_{out} = 1 - \int_{z_n>0}&\Pr(h > (I_n^1 + I_n^2 + \sigma^2)z_n^{\alpha}\beta_{nn}^{-1}T|z_n) \\ &\cdot\exp(-\pi\lambda z_n^2)2\pi\lambda z_n dz_n\end{aligned} \tag{25}$$

Fig. 3 shows that the outage probability of OAM DMN wireless network is much lower than that of frequency networking network and OAM MDM network, where OAM MDM network performed worst mainly resulting from co-mode interference caused by same mode used in different cells. The signal quality of DMN scheme 2 network is better than that of DMN scheme 1 due to the larger mode intervals among cells. When the SINR threshold is 20dB, OAM DMN method can still maintain a high quality connection.

In Fig. 4, effects of turbulence on outage probability in different schemes and λ are simulated. It can be concluded that the greater the turbulence intensity, the worse the signal quality and the greater the outage probability. For base

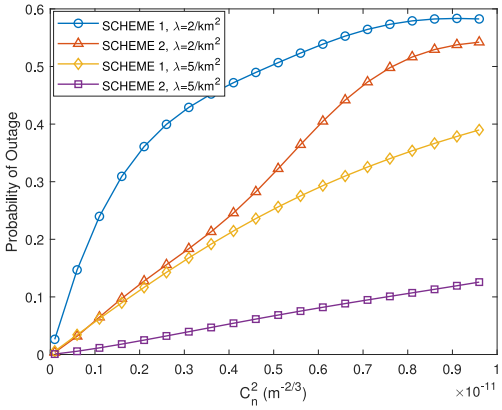

Fig. 4. The effect of turbulence on the probability of outage where T is 10dB.

station densities, outage probability of the $\lambda = 5/km^2$ situation is lower than the $\lambda = 2/km^2$ situation. We can infer that the density of the base station increases and the number of interfering cells increases, but the distance between user and base stations decreases, which reduces the OAM wave propagation distance and decreases the proportion of harmonic components of the mode expansion, thereby reducing the magnitude of inter-mode interference. Different from frequency networking, OAM DMN method has better cell signal quality with the increase of base station density.

V. Conclusion

In this letter, we proposed a OAM DMN method so as to explore the feasibility of using OAM in wireless networking. We studied atmospheric turbulence model's influence on the spiral phase of OAM wave by directly correlating with the Kolmogorov turbulence theory, which we converted turbulence into random phase screen. Taking the base station distribution and atmospheric channel into account, we got the probability density function of outage probability of OAM DMN wireless network. Simulation results showed that the proposed OAM DMN wireless network had better performance on outage probability compared with frequency networking and OAM MDM network. Besides, Compared with DMN scheme 1 and DMN scheme 2, the larger the mode interval between adjacent cells, the smaller the inter-mode interference. Furthermore, the outage probability of OAM DMN method got smaller as the base station density increased. OAM DMN can be better applied in high-density base station distribution scenario. We believed that OAM DMN had the potential for practical application in cellular network. Our future work will focus on deployment of OAM DMN into real environment with better mode allocation scheme and more specific issues of OAM including multipath, network coverage, etc.

References

[1] L. Allen, M. W. Beijersbergen, R. J. C. Spreeuw, and J. P. Woerdman, "Orbital angular momentum of light and the transformation of Laguerre-Gaussian laser modes," *Phys. Rev. A*, vol. 45, no. 11, pp. 8185–8189, 1992.

[2] Y. Yan *et al.*, "High-capacity millimetre-wave communications with orbital angular momentum multiplexing," *Nat. Commun.*, vol. 5, p. 4876, Sep. 2014.

[3] N. Zhao, X. Li, G. Li, and J. M. Kahn, "Capacity limits of spatially multiplexed free-space communication," *Nat. Photon.*, vol. 9, pp. 822–826, Nov. 2015.

[4] Y. Ren *et al.*, "Line-of-sight millimeter-wave communications using orbital angular momentum multiplexing combined with conventional spatial multiplexing," *IEEE Trans. Wireless Commun.*, vol. 16, no. 5, pp. 3151–3161, May 2017.

[5] E. Basar, "Orbital angular momentum with index modulation," *IEEE Trans. Wireless Commun.*, vol. 17, no. 3, pp. 2029–2037, Mar. 2018.

[6] T. Hu, Y. Wang, X. Liao, J. Zhang, and Q. Song, "OFDM-OAM modulation for future wireless communications," *IEEE Access*, vol. 7, pp. 59114–59125, 2019.

[7] B. Rodenburg *et al.*, "Influence of atmospheric turbulence on states of light carrying orbital angular momentum," *Opt. Lett.*, vol. 37, no. 17, pp. 3735–3737, Sep. 2012.

[8] H. Lou, X. Ge, and Q. Li, "The new purity and capacity models for the OAM-mmWave communication systems under atmospheric turbulence," *IEEE Access*, vol. 7, pp. 129988–129996, 2019.

[9] L. C. Andrews and R. L. Phillips, *Laser Beam Propagation Through Random Media*, 2nd ed. Bellingham, WA, USA: SPIE Press, 2005.

[10] E.-M. Amhoud, B. S. Ooi, and M.-S. Alouini, "A unified statistical model for atmospheric turbulence-induced fading in orbital angular momentum multiplexed FSO systems," *IEEE Trans. Wireless Commun.*, vol. 19, no. 2, pp. 888–900, Feb. 2020.

[11] B. Y. Bedir, E. E. Ebrahim, and M. A. Mahmoud, "Atmospheric turbulence mitigation using spatial mode multiplexing and modified pulse position modulation in hybrid RF/FSO orbital-angular-momentum multiplexed based on MIMO wireless communications system," *Opt. Commun.* vol. 436, pp. 197–208, Apr. 2019.

[12] B. B. Yousif and E. E. Elsayed, "Performance enhancement of an orbital-angular-momentum-multiplexed free-space optical link under atmospheric turbulence effects using spatial-mode multiplexing and hybrid diversity based on adaptive MIMO equalization," *IEEE Access*, vol. 7, pp. 84401–84412, 2019.

[13] X. Xia, K. Xu, D. Zhang, Y. Xu, and Y. Wang, "Beam-domain full-duplex massive MIMO: Realizing co-time co-frequency uplink and downlink transmission in the cellular system," *IEEE Trans. Veh. Technol.*, vol. 66, no. 10, pp. 8845–8862, Oct. 2017.

[14] A. Mahbas, H. Zhu, and J. Wang, "The optimum rate of inter-frequency scan in inter-frequency HetNets," in *Proc. IEEE Int. Conf. Commun. (ICC)*, 2017, pp. 1–6.

[15] F. Shiyao and G. Chunqing, "Influences of atmospheric turbulence effects on the orbital angular momentum spectra of vortex beams," *Photon. Res.*, vol. 4, no. 5, pp. B1–B4, 2016.

[16] W. Cheng, H. Zhang, L. Liang, H. Jing, and Z. Li, "Orbital-angular-momentum embedded massive MIMO: Achieving multiplicative spectrum-efficiency for mmWave communications," *IEEE Access*, vol. 6, pp. 2732–2745, 2018.

[17] J. G. Andrews, F. Baccelli, and R. K. Ganti, "A tractable approach to coverage and rate in cellular networks," *IEEE Trans. Commun.*, vol. 59, no. 11, pp. 3122–3134, Nov. 2011, doi: 10.1109/TCOMM.2011.100411.100541.

[18] S. M. Mohammadi *et al.*, "Orbital angular momentum in radio—A system study," *IEEE Trans. Antennas Propag.*, vol. 58, no. 2, pp. 565–572, Feb. 2010.

[19] L. Chang, Y. Yu, K. Wei, and H. Wang, "Polarization-orthogonal co-frequency dual antenna pair suitable for 5G MIMO smartphone with metallic bezels," *IEEE Trans. Antennas Propag.*, vol. 67, no. 8, pp. 5212–5220, Aug. 2019.